

> REPLACE THIS LINE WITH YOUR MANUSCRIPT ID NUMBER (DOUBLE-CLICK HERE TO EDIT) <

# Review on DFIG Supplementary SSI Damping Controllers: Design, Development, and Directions

Tao Xue, *Member, IEEE*, Ulas Karaagac, *Member, IEEE*, Mohsen Ghafouri, *Member, IEEE* and Ilhan Kocar\*, *Senior Member, IEEE*

**Abstract**—This paper presents a comprehensive review of the supplementary damping controllers (SDCs) proposed for the mitigation of sub-synchronous interaction (SSI) between doubly-fed induction generator-based wind parks (DFIG-WPs) and series capacitor compensated grids. First, the terms sub-synchronous control interaction (SSCI) and induction generator effect (IGE) are clarified by delineating their occurrence conditions and instability mechanisms in series compensated DFIG-WPs. Then, a generic design and testing framework of SDCs is proposed as a basis including the selection and adjustment of key aspects, and tests of mitigation performance, transient response and practical implementation. SDCs in the existing literature are classified into four main types considering the control structures. Their strengths and limitations are thoroughly discussed. Finally, the future directions are indicated to develop adaptive SDCs with high efficacy and robustness considering data-driven techniques.

**Index Terms**—DFIG, series capacitor compensated grids, SSI, Supplementary Damping Controllers.

## NOMENCLATURE

Phasor and error: with an arrow and with a  $\Delta$  sign  
 DFIG terminal voltage and current:  $V_i$  and  $I_i$   
 Stator voltage and current:  $V_s$  and  $I_s$   
 Stator and rotor flux linkages:  $\psi_s$  and  $\psi_r$   
 Stator resistance and leakage inductance:  $R_s$  and  $L_s$   
 Rotor resistance, leakage and mutual inductance:  $R_r$ ,  $L_r$ ,  $L_m$   
 Rotor voltage and current:  $V_r$  and  $I_r$   
 Synchronous speed and rotor speed:  $\omega_s$ ,  $\omega_r$   
 Slip and Laplace operator:  $s_{ip}$  and  $s$   
 Line current and power:  $I_{line}$  and  $P_L$   
 Series capacitor voltage and DC voltage:  $V_{cap}$  and  $V_{dc}$   
 GSC outer loop DC and AC voltage reference:  $V_{dc}^*$  and  $V_t^*$   
 GSC d- and q-axis inner loop current references  $I_d^*$  and  $I_q^*$   
 GSC and GSC modulation voltages:  $V_d^*$  and  $V_q^*$ ,  $V_{rd}^*$  and  $V_{rq}^*$   
 RSC d- and q-axis inner loop current references:  $I_{rd}^*$  and  $I_{rq}^*$   
 RSC inner current loop PI parameters:  $K_{pir}$  and  $K_{irr}$

## I. INTRODUCTION

SUB-SYNCHRONOUS oscillation (SSO) is a threat to the safe operation of wind-integrated power systems. Real-world SSO events in doubly-fed induction generator-based wind parks (DFIG-WPs) have been documented in Minnesota [1] and Texas [2] – [4] in the U.S. and Northwest China [5]. All events share two common features: (i) the DFIG-WP interacts with a series capacitor compensated grid, resulting in the occurrence of the SSO, and (ii) the oscillations have no fixed frequencies and can build up and grow rapidly. Considering the second feature, the phenomenon is named sub-synchronous control interaction (SSCI) under the umbrella of sub-synchronous interaction (SSI) to distinguish it from sub-synchronous resonance (SSR) and sub-synchronous torsional interaction (SSTI) [2], [6]. SSCI is defined as “an interaction between a power electronic control system and a transmission line in sub-synchronous frequency range” [7], which is purely electrical resonance and not related to mechanical systems. In this paper, SSCI refers to the interactions between DFIG control and the series capacitor compensated grid. However, the SSO of DFIG-WP is also considered an SSR mainly influenced by the induction generator effect (IGE) [8]. To provide clarity, the IEEE Task Force report TR-80 proposes the term “series-capacitor SSO” to describe the interactions between WPs (mainly DFIG-WP) and the series capacitor compensated grids [9]. This report explains that IGE and SSCI are “two forms” of series-capacitor SSO but does not clearly illustrate the occurrence conditions of IGE and SSCI in series capacitor compensated DFIG-WPs. Hence, this paper will use the general term SSI and delineate the boundary of SSCI and IGE.

To mitigate the SSI, optimizing control parameters [10] – [12], regulating reactive power [13], and implementing supplementary damping controllers (SDCs) [6] are proposed as possible solutions. However, the control parameters and reactive power can only be adjusted within a certain range, thus limiting the mitigation performance. Besides, tuning control parameters will also affect the transient behavior of wind turbines (WTs). Hence, converter controller parameters need to

This work was supported by the Hong Kong Research Grant Council for the Research Project under Grant 25223118.

T. Xue is with the Department of Electrical and Electronics Engineering, The Hong Kong Polytechnic University, Kowloon, Hong Kong.

U. Karaagac is with the Department of Electrical and Electronics Engineering, Middle East Technical University, Ankara, Turkey.

M. Ghafouri is with Concordia Institute for Information Systems Engineering, Concordia University, Montreal, Canada.

I. Kocar is with the Department of Electrical Engineering, Polytechnique Montreal, Montreal, Canada (email: ilhan.kocar@polymtl.ca).

> REPLACE THIS LINE WITH YOUR MANUSCRIPT ID NUMBER (DOUBLE-CLICK HERE TO EDIT) <

be designed collaboratively for damping enhancement and transient performance. The coordinated controller parameter design method overcomes the limitations of other methods (i.e., bandwidth-oriented design [14], symmetrical optimum method [15] and typical second-order system tuning method [16]) by incorporating the interactions between different controls. As an effective solution, the inner current controller and phase-locked loop (PLL) parameters are determined and validated considering adverse effects of PLL on current controls in weak grids [17], [18]. This paper focuses on SDC design and testing for instability mitigation techniques.

The early-stage SDCs originated around 2010. They are inspired from the idea of power system stabilizers (PSSs), and have a similar cascaded structure of filters, gains, and phase compensations [6]. This type of SDC is referred to as lead-lag-compensator-based SDC (LLC-SDC) in this paper. Since 2015, three new types of SDCs have been gradually developed, which are based on: observer and state feedback control (OSF-SDC) [19], virtual impedance/admittance (VIA-SDC) [20], and nonlinear control theory (NC-SDC) [21]. Besides, auxiliary devices [22], and modifying control structure are also proposed as alternative methods. Different SDCs have their own advantages and drawbacks, which will be analyzed in detail in Section IV.

While existing literature explores SSI in WPs [23] – [25], certain limitations preclude a comprehensive analysis. A broad overview of phenomena, analysis methods, instability risks across different types of WPs, and potential mitigation strategies is presented in [23], though mitigation strategies lack extensive investigation. The primary focus of [24] is the review of IGE mitigation in WPs with Type-I or Type-II WTs using flexible alternating current transmission (FACTS) devices with less emphasis on mitigation solutions for DFIG-WPs. Although SSI mitigation in WP with DFIG-WTs (Type-III WTs) by SDCs is discussed in [25], a detailed comparative analysis of different SDCs is not provided. Hence, this paper aims to bridge this gap and delves into technical details that are seldom studied in SDC research papers. Besides, the existing review papers lack a generalized design and testing procedure to inform future SDC development, which is also a void filled by this work. In summary, the contributions and contents of this paper are:

- 1) Clarify terms SSCI and IGE in series capacitor compensated DFIG-WPs by delineating their occurrence conditions and instability mechanisms (Section II).
- 2) Propose a generalized SDC design and testing procedure as a guideline and indicate/emphasize the seldom studied topics regarding transient response and practical implementation aspects (Section III).
- 3) Discuss the strengths and limitations of SDCs in the existing literature (Section IV).
- 4) Highlight future trends in which the SDCs might be effective and adaptive to mitigate different types of instabilities based on data-driven techniques (Section V).

## II. IGE AND SSCI OCCURRENCE CONDITIONS IN DFIG

When the crowbar is activated, the RSC is blocked and the

GSC is seen as an open circuit as no power flows from the RSC (see red dotted box in Fig. 1 (a)). Then the IG is directly connected to the series compensated grid, and the SSO may occur only due to the negative rotor resistance caused by the IGE (see red dotted box in Fig. 1 (b)). Therefore, the DFIG structure is similar to a Type-I or Type-II WT, and the instability under this condition is called IGE. Derivation of the simplified circuit diagram of Fig. 1 (b) can be found in [11], and the definitions of parameters are listed in the nomenclature.

During normal operation, both RSC and GSC are in service. The SSO may occur because of both the negative rotor resistance caused by the IGE and the impedance influenced by the RSC inner loop control (see red and blue dotted boxes in Fig. 1 (b)). Due to the significant impact of controls on instability, this phenomenon is called SSCI [6]. Unlike the RSC inner current loop, the RSC outer loop and the GSC controls have only marginal influence [27]. Hence, decreasing the RSC control bandwidth in a certain range is recommended to achieve the desired SSCI damping [28].

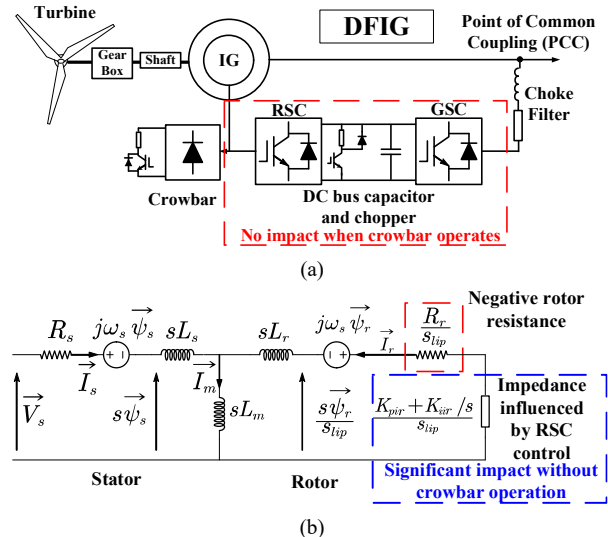


Fig. 1 Circuit explanation of SSR and SSCI terms and conditions: (a) Schematic diagram of DFIG; (b) Simplified circuit diagram of DFIG (excluding GSC and RSC outer loop impacts).

## III. A GENERIC SDC DESIGN AND TESTING SCHEME

The generic SDC design and testing scheme, shown in Fig. 2, is synthesized based on the existing work described in Section IV. The procedure also incorporates pivotal yet seldom studied topics. It is outlined beforehand to constitute a framework for evaluating the strengths and limitations of SDCs. When instability occurs, essential data is acquired including waveform records, oscillation frequency, sequence of events. Then the design and testing of SDC starts.

### A. Step 1: Selection and Adjustment of Key Elements

Three key elements of SDC include the optimal location, the control structure, and the appropriate input/output controller signal (ICS/OCS).

> REPLACE THIS LINE WITH YOUR MANUSCRIPT ID NUMBER (DOUBLE-CLICK HERE TO EDIT) <

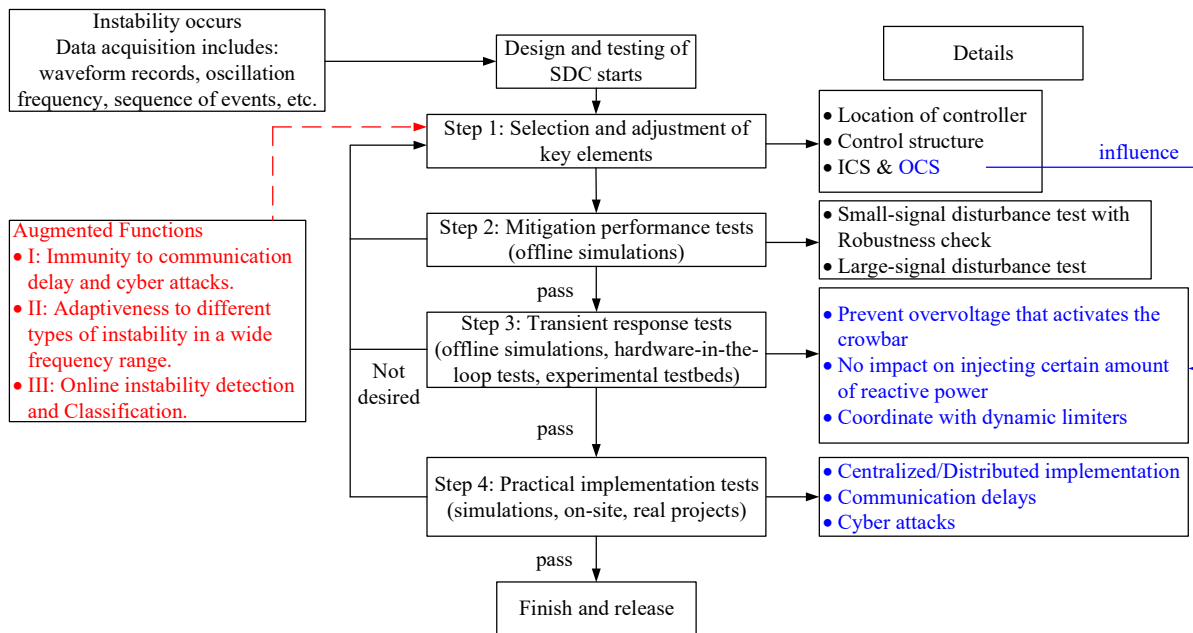


Fig. 2 The flowchart of the generic SDC design and testing scheme. Blue words: topics rarely studied in papers. Red words: augmented functions in future SDC.

### 1) Optimal Location of SDC

While there is no consensus on the optimal location for the SDC, different preferences exist. It is inserted in the q-axis RSC inner current loop by intuition (under the condition where RSC is stator flux oriented), as the RSC has a significant impact on SSI [6]. However, putting it in the GSC is also an option [30], [31]. The SDCs in either q-axis or d-axis controllers of GSC [32], [33] are proved effective by residue method to improve the damping of the system. The residue reflects the change in eigenvalue by calculating the normalized product of controllability and observability [34], which can be used to assess the damping effect and control effort of SDC. The performance of SDCs in RSC and GSC is compared in [35], and the result shows that the SDC in RSC has better damping performance, lower control effort, and better robustness against varying operating conditions. On the other hand, the impact of SDC implementation in GSC on SSI mitigation is limited to the GSC power transfer capability (up to 30% rated power). Hence, the RSC inner loop is recommended as the optimal location, which is then widely acknowledged in most VIA-SDC designs which will be shown later in Section IV. C.

### 2) Control Structure of SDC

The structure of SDC depends on the control theory. The SDCs in existing works can be classified into four types: LLC-SDC, OSF-SDC, VIA-SDC, and NC-SDC as mentioned in the Introduction section. The SSI mitigation mechanisms of those SDCs will be illustrated in Section IV.

### 3) ICS and OCS Selection

The ICS selection is an important design step in developing control systems. This was extensively examined in early foundational studies, while more recent works typically adopt prevailing conclusions from earlier literature or omit explicit discussion. On the other hand, while intrinsically linked to the transient response characteristics, explicit examination of the OCS selection remains scarce in the literature. Its selection will

be discussed in detail in Section III. C. A classic method to select both ICS and OCS is to calculate the controllability and observability of the linear system. Control efforts are reduced when the variables with large controllability and observability are selected as OCS and ICS, respectively. In [36], the active power is calculated to have the largest observability, so it is selected as the ICS, and the rotor voltage has the largest controllability, so it is selected as the OCS. The ICS and OCS selections in [36] align with the early research work described in [6] with the sole divergence being ICS (active power error is used in [6] while the active power is used in [36]). The residue method can also be used to pair ICS and OCS in designing the LLC-SDC, as a higher magnitude of the residue results in less control effort and a lower phase lead/lag of the residue results in less phase compensation effort [37]. Another way to select the ICS is to choose the state variables with higher Hankel Singular Values (HSVs) [38]. The HSV reflects the energy of each state in the system, and the states with the larger energy represent most of the system's characteristics in terms of stability, frequency, and time response.

### B. Step 2: Mitigation Performance tests

The mitigation performance tests include small-signal and large-signal disturbance tests [36], and are usually conducted in offline simulations. The small-signal disturbance test is usually conducted on a linearized system state-space model together with a robustness check. Eigenvalues reflecting the SSI mode are observed under different wind speeds, series compensation levels, system load types, and demands [36], [40]. The design of SDC should ensure that the eigenvalues stay in the left-half plane under all possible operating conditions. The large-signal disturbance test is usually conducted with electromagnetic transient level (EMT-level) time domain simulations. The DFIG-WP will be left radially connected to series capacitor compensated grids after a fault, and different fault types, fault

> REPLACE THIS LINE WITH YOUR MANUSCRIPT ID NUMBER (DOUBLE-CLICK HERE TO EDIT) <

distances, and fault durations can be used to check the SDC performance [40]. The after-fault operating conditions can be selected like the small-signal disturbance test scenarios, so that the corresponding results in two tests can match each other. Two disturbance tests are designed in this manner in [36].

### C. Step 3: Transient Response Tests

The OCS selection has a significant impact on the transient response, but it is not considered if the OCS design is only based on controllability. If the modulation voltage is selected as the OCS, then a large OCS value in transients may lead to overvoltage that activates crowbar operation. Inner current loop references (output of outer control loops) are preferable, as they are usually implemented with dynamic limiters to achieve the desired transient response and fulfil grid codes [39], [40].

During normal operation, priority is given to the active current injection, and the reactive current will be limited, as shown in Fig. 3. The active current reference  $I_{ac}^*$  is limited to the active current limit  $I_{aclim}$  (within the circle):

$$I_{ac}^* < I_{aclim} \quad (1 \text{ pu}) \quad (1)$$

The reactive current reference  $I_{re}^*$  is limited to the reactive current limit  $I_{relim}$  determine by the dynamic limiting scheme:

$$I_{re}^* < I_{relim} = \sqrt{I_{lim}^2 - (I_{ac}^*)^2} \quad (I_{lim} = 1.1 \text{ pu}) \quad (2)$$

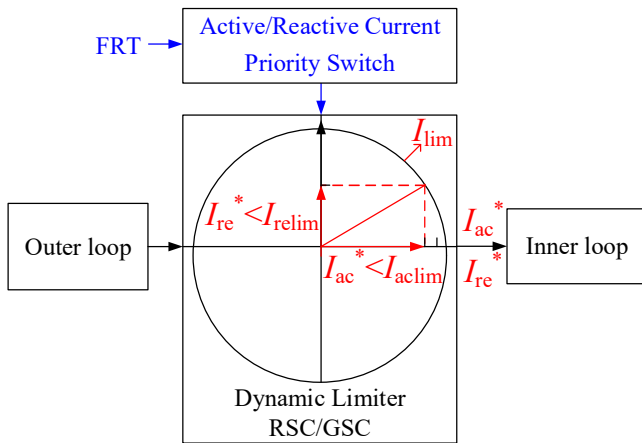


Fig. 3 Dynamic limiter implementation for inner current loop references (normal operation).

When the FRT function is activated under fault scenarios, the priority is given to the reactive current injection, thus reversing the current dynamic limiting scheme in (1) and (2). For stator flux-oriented RSC control, the active current is at q-axis and the reactive current is at d-axis. For stator voltage-oriented RSC control, the corresponding relationship will be the opposite. The remaining reserves of active and reactive currents can be given to the output of SDC, and similar dynamic limiter can also be augmented to the sum of outer loop control output and SDC output (see Fig. 8 (b) later). In this manner, the SDC will not influence the transient response of the DFIG to fulfil the grid code requirements. Besides, the dynamic limiting approach in [40] also shows superior damping performance than blocking SDC during faults [41].

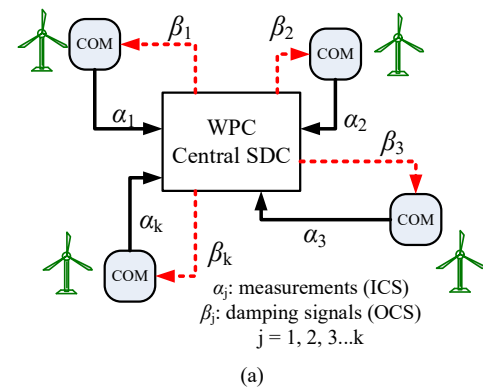
The dynamic limiting approach sets current limits, additional controls are required to improve the DFIG transient behavior and prevent oscillations during grid faults such as RSC inductance-emulating control for mitigating postfault rotor overcurrent [42] and feedforward current references control for tracking ability enhancement [43]. The over-modulation issue under asymmetrical faults is a cause of oscillations. A control solution encompassing transient flux linkage observer, transient voltage and current calculators is proposed as a solution that also maintains positive- and negative-sequence reactive currents per grid code requirements [44].

Transient response tests are advised as necessary tests in SDC design, which can be conducted in offline simulations, hardware-in-the-loop (HIL) simulations, and on experimental testbeds. This ensures grid reliability when implementing SDCs during transients.

### D. Step 4: Practical Implementation Tests

Most SDCs are designed based on simplified DFIG-WP model, so the mitigation performance may not be guaranteed in practice. Nonlinearities (dynamic limiters of inner loop current references, converter saturation, etc.), FRT functions and reactive power controller at the wind park controller (WPC) should be considered in a detailed DFIG-WP model [45]. Hence, the mitigation performance of SDC needs to be validated by EMT-level simulations with the detailed model.

SDCs are typically designed and embedded in the WP level (called central implementation in WPC as shown in Fig. 4 (a)). Centralized implementation relies on the high-resolution data transfer of the communication networks between the WPC and individual DFIGs. The SDC in WPC receives measurements  $\alpha_j$  (i.e., voltages) as ICS, and outputs damping signals  $\beta_j$  (i.e., currents) to WTs as OCS. The SDC performance can be significantly deteriorated due to the communication delays in practice. A Smith Predictor scheme based SDC can be utilized as countermeasure against communication delays to maintain the normal function of SDCs [46]. An alternative distributed implementation proposed in [47] is not vulnerable to the mentioned communication network latency issues as the SDC is integrated into the DFIG-WT control and receives only the WT outage information updates from the WPC to improve the mitigation performance [47], as shown in Fig. 4 (b).  $N$  is the number of WTs in service. ICS and OCS are generated in local SDCs.



(a)

> REPLACE THIS LINE WITH YOUR MANUSCRIPT ID NUMBER (DOUBLE-CLICK HERE TO EDIT) <

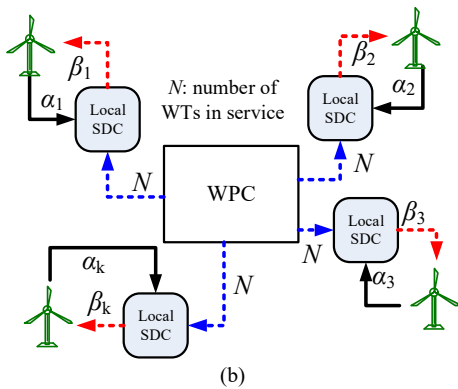


Fig. 4 SDC practical implementation schemes: (a) centralized, (b) distributed.

The dependency on cyber systems also makes the DFIG-WP prone to cyber threats [48], as shown in Fig. 5. The internal cyber-attacks target the WPC, which may create long communication latency or deliver wrong signal packages. The external cyber-attacks target the external grid, which may cause tripping of switch and leads to the WP radial connection to series-capacitor compensated grid (SSI risk). A robust state observer is designed to detect internal cyber-attacks and remove wrong signals, and a robust static-output feedback SDC is designed for SSI mitigation under external cyber-attacks [48]. Hence, immunity to communication delay and cyber-attacks is proposed as the Augmented Function I in Fig. 2. Last but not least, the practical implementation tests are recommended as the final step, which can be conducted in offline simulations and on-site in real projects. This ensures the reliability of SDC performance in real working conditions of WPs.

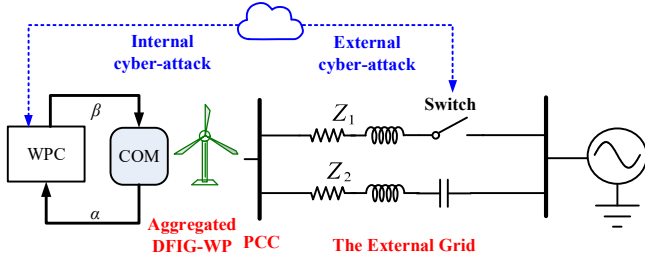


Fig. 5 The internal and external cyber-attacks.

#### IV. EVALUATION OF THE SDCs IN EXISTING LITERATURE

The strengths and limitations of four main types of SDCs will be evaluated based on the proposed framework in Section III.

##### A. Lead-Lag Compensator based SDC (LLC-SDC)

A typical control structure of an LLC-SDC is shown in Fig. 6, including gain, wash-out block, bandpass filter, and phase compensation. The LLC-SDC is inspired by the idea of a PSS and the bandpass filter is not a compulsory block but can improve the performance of the LLC-SDC. The gain  $K$  determines the damping provided by the LLC-SDC. The wash-out block is a high-pass filter to filter out the steady-state components [32]. The second-order bandpass filter (BPF) extracts the sub-synchronous component by setting the center frequency  $\omega_c$  as the sub-synchronous frequency  $\omega_{sub}$  or its complement of fundamental frequency ( $\omega_0 - \omega_{sub}$ , it depends on whether the ICS and OCS are in the dq domain or abc

domain, etc.). The damping coefficient  $\zeta$  is proportional to the bandwidth, and a smaller bandwidth results in a better effect of extracting center frequency but less tolerant to the deviation of the oscillation frequency. The phase compensation block consists of one or more (denoted as the index  $m$ ) cascaded blocks with similar transfer functions. The time constants  $T_1$  and  $T_2$  can be adjusted by the classic residue method [36] or the advanced optimization algorithms like the particle swarm optimization (PSO) technique [49] to compensate for the phase lead/lag of the ICS and OCS.

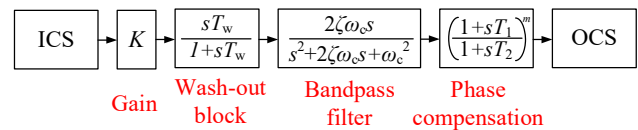


Fig. 6 A typical control structure of an LLC-SDC

The ICS, OCS, and control structure of some typical LLC-SDCs in existing literature are listed in TABLE I. The ICS is usually selected from  $\omega_t$ ,  $P_L$ ,  $I_{line}$ , and  $V_{cap}$ . However,  $\omega_t$  or  $\Delta\omega_t$  is not a good selection as it has low observability. A high gain  $K$  is needed to ensure the damping improvement, but it may also lead to instability of other modes [50].  $P_L$  and  $I_{line}$  with high observability [37] can be measured at WP substation, so they can be considered as local measurements in SDC implementation [41]. The  $V_{cap}$  is also found to be an effective ICS in [50], but it cannot be measured locally and should be approximated by  $I_{line}$  [31]. The OCS selection and SDC location have been discussed in Section III, and SDC implemented in RSC and OCS added to inner loop current references are recommended. However, most studies take GSC as SDC location, and OCS for modulation voltages. This is not preferred for future SDC designs.

TABLE I  
ICS, OCS, AND CONTROL STRUCTURE OF THE LLC-SDCS

Papers and years	ICS	Structure	OCS
[6] 2010	$\Delta\omega_t$	No wash-out and BPF	$V_{rq}^*$ (RSC)
[30] 2010	$\Delta\omega_t$	N/A	$V_t^*$ (GSC)
[31] 2012	$I_{line}$ or $V_{cap}$	N/A	$V_{dc}^*$ (GSC)
[37] 2012	$I_{line}$ or $P_L$	N/A	$I_q^*$ (GSC)
[41] 2014	$I_{line}$ or $P_L$	All	$I_q^*$ (GSC)
[32] 2015 [50] 2015	$\omega_t$ , $P_L$ or $V_{cap}$	No BPF	$V_t^*$ , $I_q^*$ , or $V_q^*$ (GSC)
[36] 2016	$P_L$	No wash-out block	$V_{rq}^*$ (RSC)
[49] 2016	$\omega_t$	All	$V_{rd}^*$ , $V_{rq}^*$ (RSC)
[51] 2017	$P_L$	No BPF	$V_d^*$ , $V_q^*$ (GSC)
[52] 2018	$\Delta V_{dc}$	No BPF	$I_q^*$ (GSC)
[53] 2018	$\Delta\omega_t$	No wash-out block	$V_{rd}^*$ (RSC)
[54] 2020	$V_{cap}$	No BPF	$V_t^*$ (GSC)

> REPLACE THIS LINE WITH YOUR MANUSCRIPT ID NUMBER (DOUBLE-CLICK HERE TO EDIT) <

### B. Observed State Feedback based SDC (OSF-SDC)

A typical control structure of an OSF-SDC is shown in Fig. 7. The OSF-SDC design includes system model reduction, state observer gain design, and state feedback gain design. The damping mechanism relies on the state feedback loop (indicated by green words in Fig. 7), and the feedback gain matrix  $-\mathbf{K}_{damp}$  can be designed by optimal quadratic technique (this method is also called linear quadratic regulator, LQR) [55]. The cost function  $J = \int (\mathbf{y}^T \mathbf{Q} \mathbf{y} + \mathbf{u}^T \mathbf{R} \mathbf{u}) dt$  is minimized to calculate  $-\mathbf{K}_{damp}$ , where the matrices  $\mathbf{Q}$  and  $\mathbf{R}$  can be selected to represent a tradeoff between control energy spent by control output ( $\mathbf{y}$ ) and control actuators ( $\mathbf{u}$ ) [35]. The state feedback uses the estimated internal states ( $\mathbf{x}_r$ ) of the reduced order model rather than the real state variables ( $\mathbf{x}$ ). Those internal states have no physical meaning and cannot be measured. Hence, the internal states should be obtained through a low-order approximation neglecting state variables that have marginal effects on the SSI mode damping [19]. The reduced order model can be obtained by balanced model truncation using Schur method [56]. The state observer gain matrix  $\mathbf{K}_{ob}$  can also be designed by LQR method like designing  $-\mathbf{K}_{damp}$  [35], [38], [57], eigenvalue placement by linear matrix inequality (LMI) method [40], [45], and Kalman filter [55].

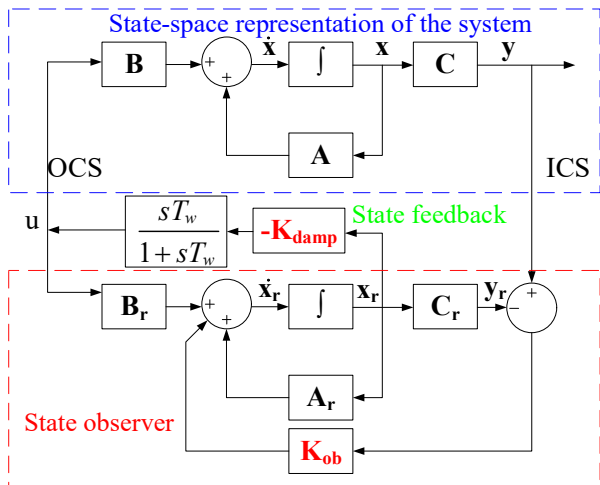


Fig. 7 The state-space representation, the state observer, and the state feedback (control law) of the system.

The ICS and OCS selection of some typical OSF-SDCs in existing literature are listed in TABLE II. Local measurements like stator currents  $I_{sdq}$ , rotor currents  $I_{rdq}$  (equal RSC currents), GSC currents  $I_{dq}$ , or their combinations are selected as the ICS. Ref. [35], [38] select RSC modulation voltage  $V_{rdq}^*$  and Ref. [57] selects GSC outer loop AC voltage reference  $V_t^*$  as the OCS, which might cause overvoltage issues as discussed in section III. It is not recommended if not equipped with extra voltage limiters. The inner loop current references are chosen as OCS in [40], [47], so that the DFIG with SDC implementation can achieve the desired transient response, which is advised in practice.

TABLE II  
ICS AND OCS OF THE OSF-SDCS

Papers and Time	ICS	OCS
[38] 2015	$I_{sdq}$	$V_{rdq}^*$ (RSC)
[57] 2015	$I_{sdq}$	$V_t^*$ (GSC)
[35] 2015	$I_{sdq}, I_{rdq}$	$V_{rdq}^*$ (RSC)
[40] 2017 [47] 2019	$I_{rdq}, I_{dq}$	$I_{rdq}^*$ (RSC), $I_{dq}^*$ (GSC)

### C. Virtual Impedance/Admittance based SDC (VIA-SDC)

A typical control structure of the VIA-SDC is shown in Fig. 8, which includes two main types: virtual impedance (VI-SDC) and virtual admittance (VA-SDC). Both VI-SDC and VA-SDC can be implemented in the RSC or GSC and can operate at dq- or abc-frame (Implementation in RSC and operation at dq-frame is presented as an example in Fig. 8). The ICS and OCS selections are fixed, if ICS is current and OCS is voltage then it is classified into VI-SDC, if opposite then it is VA-SDC. There is also a third version called harmonic voltage/current compensation (HVC/HCC) by selecting voltage/current both for ICS and OCS, which is omitted here for simplicity.

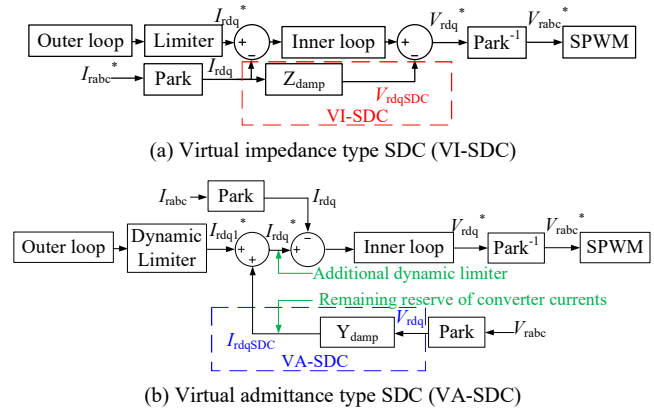


Fig. 8 Typical structure of the VIA-SDC.

SSI mitigation by VI-SDC (VA-SDC) is through a series (parallel) connection of impedance (admittance) at the output terminal of RSC to absorb the oscillation energy [58], which is shown in Fig. 9. The impedance  $Z_{damp}$  (admittance  $Y_{damp}$ ) is usually comprised of a filter and a PID controller. The filter can be a bandpass, band stop, lowpass, and high pass filter (denoted as BPF, BSF, LPF, and HPF, respectively) or their combinations, with the function of extracting the oscillation frequency component from the ICS. Then, according to the definition of impedance and admittance, the P, I, and D controllers represent virtual resistance, capacitance, and inductance in VI-SDC, while they represent virtual conductance, inductance, and capacitance in VA-SDC. Hence, the VI-SDC mitigates the instability by a voltage drop in  $Z_{damp}$  containing the oscillation frequency component, and the VA-SDC mitigates the instability by a current flow containing the oscillation frequency component through  $Y_{damp}$ .

> REPLACE THIS LINE WITH YOUR MANUSCRIPT ID NUMBER (DOUBLE-CLICK HERE TO EDIT) <

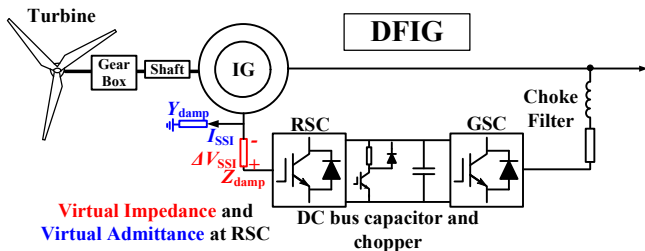


Fig. 9 Circuit explanation of Virtual impedance and virtual admittance implementation in DFIG.

The control structures of some typical VIA-SDC in existing works are listed in TABLE III. It can be seen that most works ([59] – [64], [66] – [68]) select RSC to implement the VI type SDC. Implementation in the d-axis rather than q-axis of the RSC [61], using VI-SDC rather than HVC [62], and using virtual capacitance (I controller) rather than virtual resistance (P controller) of VI-SDC [64] are proved to have better mitigation effects than their counterparts. The mitigation effects of the VIA-SDC are often explained by impedance-based stability analysis (IBSA) as improving the phase margin (seen in the Bode diagram) [58] or increasing the system resistance (seen in the R-X diagram) [62]. The parameters of the virtual impedance/admittance (represented by PID controller) can also be optimized using the genetic algorithm [63], [66].

However, the current design of VIA-SDC lacks testing transient performance. Most existing works select VI-SDC rather than VA-SDC as the main type, thus may lead to overvoltage conditions with modulation voltage as OCS. The VA-SDC can select inner loop current references as the OCS, so the transient response can be ensured by implementing an additional dynamic limiter as a secondary limiting module in series with the existing limiter of the outer loop, as shown in Fig. 8. The amount of VA-SDC output currents is determined by the remaining reserve of converter currents, which can be improved by implementing insulated gate bipolar transistors (IGBTs) with higher overcurrent ability. As the VI-SDC and VA-SDC are comparable in terms of mitigation performance [58], the VA-SDC is preferred with the consideration of the transient performance.

TABLE III  
CONTROL STRUCTURES OF THE EXISTING VIA-SDCS

Paper and Time	Type	Control Structure and Location
[58] 2015	VI, VA	BPF (GSC)
[59] 2015	VI	D controller +LPF+ phase compensation (RSC)
[60] [61] 2015	VI	BSF (RSC)
[62] 2016	HVC	BSF (RSC)
[63] 2018	VI	BPF+PI controller (RSC)
[64] 2019	VI	BPF+I controller (RSC)
[65] 2020	VI	HPF+P controller (GSC)
[66] 2021	VI	BSF+BPF+HPF+PD controller (RSC)
[67] 2021	VI	HPF (RSC)
[68] 2021	VI	HPF+PD controller (RSC)

#### D. Nonlinear Controller based SDC (NC-SDC)

The NC-SDC can be implemented on the RSC or GSC control by two strategies: substituting the existing PI controller or adding to the existing PI controller. The substitution type of

NC-SDC [72], [73], [75] – [77] should also be responsible for the normal operation of converters, while the add-on type of NC-SDC [21], [46], [48], [69] – [71], [74], only serves for SSI mitigation. The ICS, OCS, controller type, and implementation strategy in existing works are listed in TABLE IV.

TABLE IV  
ICS, OCS, CONTROLLER TYPE AND IMPLEMENTATION OF THE NC-SDCS

Paper and Time	Controller Type and Implementation	ICS	OCS
[21] 2016 [69] 2017	Partial feedback linearizing (PFL) (Add-on, GSC)	Output of inner loop PI controller	$V_{rdq}^*$ , $V_{dq}^*$
[70] 2018	$H_\infty$ controller (Add-on, RSC)	$\Delta I_{rdq}^*$	$V_{rdq}^*$
[71] 2019	PFL and Exact feedback linearizing (EFL) (Add-on, RSC & GSC)	Output of inner loop PI controller	$V_{rdq}^*$ , $V_{dq}^*$
[72] 2019 [73] 2019	Sliding mode controller (Substitution, RSC & GSC)	$V_{cap}$	$V_{rdq}^*$ , $V_{dq}^*$
[74] 2019 [46] 2021	$\mu$ controller (Add-on, RSC & GSC)	$I_{sdq}$ , $I_{dq}$	$I_{rdq}^*$ , $I_{dq}^*$
[75] 2020	Active disturbance rejection controller (Substitution, RSC)	$\Delta I_{rdq}^*$	$V_{rdq}^*$
[76] 2020	Sliding mode controller (Substitution, RSC)	$I_{rdq}^*$	$V_{rdq}^*$
[77] 2021	Energy-shaping (Substitution, RSC)	$I_{rdq}^*$ , $I_{sdq}^*$	$V_{rdq}^*$
[48] 2021	Static-output feedback (Add-on, RSC & GSC)	$I_{sdq}$ , $I_{dq}$	$I_{rdq}^*$ , $I_{dq}^*$

The rotor, stator, or converter currents from the local measurements are the ICS and the modulation voltages are the OCS in most of the existing literature. The reason for the OCS selection is that the output of substitution type NC-SDC must be the modulation voltages for the sinusoidal pulse width modulation (SPWM). An extra voltage limiter is implemented to prevent overvoltage issues of substitution type NC-SDC in [76]. However, the add-on type of NC-SDC can be modified by selecting inner loop current references as the OCS.

#### E. SDC in Auxiliary Devices

Auxiliary devices can also be utilized to mitigate SSI. This idea originates from using FACTS devices to mitigate SSR in WPs with Type-I or Type-II WTs. FACTS devices already existed in the WP medium voltage bus, so they only need a software update incorporating SDC functions. FACTS devices used for SSR mitigation include static var compensator (SVC) [78], [79], static synchronous compensator (STATCOM) [80], [81], thyristor/gate turn-off thyristor (GTO) controlled switched capacitors (TCSC/GCSC) controlling line impedances [82], [83], and unified power flow controller (UPFC) [84]. Other works related to FACTS mitigating SSR can be found in the review paper [24].

There are synergies between SDCs and other grid technologies. SDC can be either a software update to existing grid devices, or a main function of auxiliary devices for SSI mitigation. The auxiliary devices can be connected at the point of interconnection (PoI) of the WP, but they need extra investments. The mechanism is to use the auxiliary devices to

> REPLACE THIS LINE WITH YOUR MANUSCRIPT ID NUMBER (DOUBLE-CLICK HERE TO EDIT) <

absorb the oscillation energy, so the ratings of auxiliary device capacity are the key considerations. The type of SDC and the ratings of auxiliary devices in existing works are listed in TABLE V. The above-introduced LLC-SDC, VIA-SDC, and OSF-SDC are utilized in these auxiliary devices. The ratio of the device over WP capacity ranges from 0.17% to above 100%, as they are designed under different operating conditions. For ratios less than 1% [84] – [87], the auxiliary devices aim at mitigating SSI in low wind speed scenarios (less than 10% WP output power). For MMC station [88] and SVC [92], their main functions are not SSI mitigation, so their capacities can be very large. For the VSC with BESS [89], [90], their capacities depend on the investments.

TABLE V  
SDC TYPES AND RATINGS OF AUXILIARY DEVICES IN EXISTING WORKS

Paper Time	SDC type	Rating and ratio of WP capacity
Cascaded H-bridge converter		
[84] 2015	VA-SDC	5MVA/3000MVA (0.17%)
[86] 2019	VA-, HCC-SDC	12MVA/2400MW (0.5%)
[87] 2020	VA-, HCC-SDC	10MVA/2000MW (0.5%)
MMC station		
[88] 2021	OSF-SDC	500-2500MW (>100%)
VSC with BESS		
[89] 2021	PI controller	10MW/9MW (111%)
[90] 2022	VA-SDC	30MW/100MW (30%)
SVC with SDC implementation		
[91] 2012	LLC-SDC	N/A
[92] 2014	LLC-SDC	120MVA inductive & 100MVA capacitive/1224 MW (10% & 8%)
[93] 2017	VA-SDC	N/A

#### F. Modifying Control Structure

Eliminating the RSC inner current loop is proposed to minimize the impact of negative resistance on SSI [94]. However, it abandons the current limit functions of RSC and may lead to converter overcurrent under fault conditions. Virtual synchronous generator (VSG) control substituting the RSC PI controllers in [95] may also be a solution by providing positive resistance in sub-synchronous frequency range. Resonant controller is also proposed to control the oscillation component of the current utilizing the advantage of following sinusoidal references [96]. A new term of “motion-induction amplification” is proposed in [97] to explain that the root cause of SSI originates from the speed voltage term of the rotor (see  $j\omega_r \overline{\psi}_r$  in Fig. 1) and the elimination technique of this term is improved in [98]. However, these works need further verification as the established understanding of the SSI root-cause is the negative impedance influenced by the RSC control rather than the speed voltage term [6].

#### G. Performance Comparison of SDCs and Selection Guide

Performance of the four main SDCs is compared in TABLE VI. The wind speed comprises of all the working conditions in existing SDCs, and compensation level is concluded from the optimal SDC ability in each type, and the properties are distinct functions in each literature.

The LLC-SDC is a preliminary solution to SSI in the first stage as it is easy to design and implement. The mitigation is

achieved through simple feedback control, so its effectiveness is guaranteed only in one specific operating point in 6 – 13 m/s wind speed with no more than 85% compensation levels [51]. Ref. [49], [50], and [52] – [54] discuss tuning the parameters of the LLC-SDC to improve its robustness when small deviations exist in wind speeds and compensation levels. An adaptive control idea of gain scheduling is also proposed in [50] and [54] to design a lookup table for the gain of the LLC-SDC. However, those works only consider radial connection DFIG-WP to a single series capacitor compensated line.

The OSF-SDC can be regarded as an improvement of the LLC-SDC, as the mitigation of the OSF-SDC is similar to the LLC-SDC by using feedback control. However, its performance highly depends on the accuracy of the reduced-order model. This can be solved by augmenting the order of that model, but it increases the complexity of the control design, opposing the initial objective. In general, it improves robustness by using the internal states to represent the main dynamics of the system, so it is effective in varying operating points in 3.25 – 9.75 m/s with no more than 75% compensation level [35] (a little narrower range than LLC-SDC). However, the OSF-SDC can handle larger oscillation frequency deviations due to multiple compensated line outages [47].

The VIA-SDC can work in varying operating points in 3.5 – 11 m/s with no more than 90% compensation level [64] and enhance the FRT performance simultaneously [59]. However, the dissipation of oscillation energy through the virtual impedance/admittance in the DFIG model raises physical concerns, as the ultimate sink for this energy in a real system remains unspecified. Hence, VIA-SDC is theoretically effective but needs practical experiments and validations (a practical example is presented in [66]). Furthermore, the mitigation efficacy of VIA-SDC highly depends on the frequency extraction function of the filter. Hence, improving the responsiveness of the filter across a wider frequency range presents an area for future enhancements.

NC-SDC has competitive performance than other linear SDCs, which is effective in 5 – 12 m/s wind speed with no more than 90% compensation level [77]. Except for adaptability in multiple compensated line outages [46], NC-SDCs boost the disturbance rejection ability to changes in external environment. Hence, the SDC robustness are significantly improved by employing different nonlinear control theories. The sliding mode controller remains effective when DFIG electrical parameters decrease by 50% [72], or GSC filter parameters vary by 20% [73]. The  $\mu$  controller is robust when the line resistance, inductance and capacitance varies by 30%, 17% and 17% [74], and the Hamilton energy shaping controller exhibits similar properties by addressing 25% – 50% increase of line inductance [77]. The other NC-SDCs include EFL/PFL control [21], [69], [71],  $H_\infty$  controller [70], the active disturbance rejection controller (ADRC) [75] and the static output feedback controller [48]. However, the NC-SDC increases the complexity of design and the computation burden of the hardware controller in practice, so it is not widely used.

> REPLACE THIS LINE WITH YOUR MANUSCRIPT ID NUMBER (DOUBLE-CLICK HERE TO EDIT) <

TABLE VI  
PERFORMANCE COMPARISON OF LLC-, OSF-, VIA- AND NC-SDCS

SDC-Type	Effective Operating Region	Wind Speed	Compensation Level	Properties
LLC-SDC	One specific operating point with small deviations	6 – 13 m/s	≤ 85% [51]	Radial compensated line
OSF-SDC	Varying operating points	3.25 – 9.75 m/s	≤ 75% [35]	Multiple compensated lines [47]
VIA-SDC	Varying operating points	3.5 – 11 m/s	≤ 90% [64]	a. Radial compensated line b. FRT performance improvement [59] c. Unverified physical issue d. Reliance on frequency extraction filters
NC-SDC	Varying operating points	5 – 12 m/s	≤ 90% [77]	a. Multiple compensated lines [46] b. Robustness further improves when: • DFIG parameter ↓50% [72] • GSC filter parameter ±20% [73] • Line R X <sub>L</sub> X <sub>C</sub> varies 30%, 17%, 17% [74] • Line X <sub>L</sub> ↑ 25% – 50% [77] c. Complex design and computation burden

The potential concern of SDCs in auxiliary devices is the additional costs and cyber threats. Auxiliary devices need to be carefully considered for SSI mitigation, as this involves extra investments which is not preferred by the manufacturers. On the other hand, using the existing devices in the system with SDC software implementation needs efficient communication with the WPC, which can be easily influenced by network latency and cyber-attacks. Those devices need to shift from their normal operation to SSI mitigation after receiving the SSI emergency order from the WPC. Modification of control structures provides insights to instability phenomenon but requires further investigations.

#### V. FUTURE TRENDS OF SDC

The DFIG not only faces SSI risk (in sub-synchronous range). Weak grid instability risk (in super-synchronous range) of DFIG-WP is also predicted in [99], [100], and confirmed by real-world incidents in Northwest China [101], [102]. Hence, adaptiveness to different instabilities of inverter-based resources (IBRs), and online instability detection and classification are proposed as the Augmented Functions II and III in Fig. 2. A promising future direction is to design data-driven and machine learning-based techniques to mitigate the instabilities in a WP, a highly uncertain and time-varying plant. These data-driven controllers can (i) replace one of the wind park conventional control structures, e.g., RSC inner loops due to their significant impact on the SSI, or (ii) be used to design the SDCs, which are integrated into the RSC and GSC control loops. Such controllers have been previously used in various power system applications, e.g., transient stability improvement of WPs [103], permanent magnet motors [104], power electronic converters [105], transient stability improvement [106], low voltage ride through [106], and MPPT performance [108].

Application of data-driven SDC in conventional SG-based power system stability has been studied for decades. Reinforcement learning (RL) [109] is commonly employed in these control scenarios, as the learning process bears similarity to the interaction between a controller and control plant [110]. The foundational study of RL in power system stability arised

around two decades ago [111], introducing an ideal online and a practical offline mode to train and apply the RL-based agent (RL-Agent) to damp the inter-area oscillations. RL-Agents are trained to adjust the thyristor controlled switched capacitor (TCSC) [112], the resistor damper [113], the power system stabilizer (PSS) [114] and replace the wide-area damping controller [115], [116]. However, the early-stage studies mainly focus on a two area four machine system [29], as the damping performance is limited by the RL-Agent output in discrete action spaces. In recent years, the performance and efficiency of RL have been improved with the development of deep learning [117]. The deep RL-Agent (DRL-Agent) works in continuous action spaces [118], and is capable of stabilizing inter-area oscillations in the IEEE 10 machine 39 bus system [119], 16 machine 68 bus system [120], and adjusting several PSSs simultaneously [121]. DRL can also be coordinated with deep supervised learning to enhance system stability under different operating conditions [122].

However, the applications in mitigating SSI or weak grid instability have just been initiated and require further investigations. Current challenges include but not limited to:

- 1) DRL-Agent implementation in IBRs. Due to distinct control and protection strategies of IBRs compared to conventional SGs, the location, control structure, ICS and OCS of the DRL-Agent need to be elaborately re-designed.
- 2) Training, validation and testing scheme design. Provided that data of the wind park encompassing real-world incidents is accessible from simulations or historical measurements, a huge dataset is available. A general and systematic scheme needs to be specified to guide the use of the dataset in the three fundamental procedures of DRL.
- 3) Training time increase. Unlike the inter-area oscillations simulated in electro-mechanic transient timescales, conducting two computationally intensive works simultaneously (EMT simulation and DRL training) is a heavy burden for a single CPU. Parallel computing of several CPUs, high computing speed of GPU, real time simulations can provide promising solutions.
- 4) Trust from the system operators. Although data-driven SDCs might be more effective and adaptive than

> REPLACE THIS LINE WITH YOUR MANUSCRIPT ID NUMBER (DOUBLE-CLICK HERE TO EDIT) <

conventional SDCs, their solutions might be challenging to interpret. Hence, physics-informed artificial intelligence (AI) [123] incorporates the human-knowledge accumulated in centuries with the advanced computational machine learning algorithms, and it may provide reliable solutions for system operators to trust.

## VI. CONCLUSIONS

This paper has provided a comprehensive review of the design, development, and future directions of SDCs for mitigating SSI in DFIG-WPs. The paper first delineates the mechanisms and occurrence criteria distinguishing IGE and SSCI instabilities. The latter represents the more prevalent SSI as events predominantly occur without crowbar activation.

Through detailed analysis of prior works, a generalized SDC design framework is derived to assist readers in engineering their SDC designs. The synthesized methodology presented in this paper can serve as a basis to evaluate the strengths and limitations of the existing designs. Recommendations of this paper are provided as a reference:

- 1) The location of SDC is recommended in RSC rather than GSC to ensure better damping performance, lower control effort, higher power transfer capability, and improved robustness against varying operating conditions.
- 2) Four main types of controllers demonstrate distinct advantages and limitations: LLC-SDC is suitable for one specific operating point while OSF-SDC can handle varying operating conditions. VIA-SDC is theoretically effective and can also improve FRT performance but needs practical experiments and validations. Advanced NC-SDC is robust but may increase the computational burden. Alternative approaches like auxiliary devices depend on capacity and require extra investments, while control structure modifications show promise but need further investigation.
- 3) Signals with high observability are recommended as ICS, while those with high controllability should serve as OCS. For optimal wind turbine transient performance, inner loop current references with dynamic limiters (controlled by the outer loop) are more effective as OCS compared to modulation voltages.
- 4) Future SDC tests require rigorous assessment of transient performance and practical implementation considerations. To achieve this, close collaboration between academia and industry will be essential.

Proposed future avenues, including immunity to communication delays and cyber-attacks, adaptive wide frequency range operation, integrated detection, classification, and compatibility with the transient response of converters are discussed to guide further investigations. Data-driven methods like physics-informed AI may prove promising to achieve resilient SDCs. By addressing the identified challenges and knowledge gaps, SDCs can fulfill stability needs in modern power electronics-based grids.

## REFERENCES

- [1] A. Mulawarman and P. G. Mysore, "Detection of Undamped Sub-Synchronous Oscillations of Wind Generators with Series Compensated Lines," in *Minnesota Power Systems Conference*, 2011, pp. 1–5.
- [2] G. D. Irwin, "Sub-Synchronous Interactions with Wind Turbines," in *Technical Conference - CREZ System Design and Operation*, Jan. 2010.
- [3] A. K. Jindal, G. D. Irwin, and D. A. Woodford, "Sub-synchronous interactions with wind farms connected near series compensated AC lines," in *Workshop on large scale integration of wind*, Oct. 2010, pp. 559–564.
- [4] R.O. Keefe, E. Rezaei, K. Andov, et al. "Simulation of 2017 wind farms into series capacitor sub-synchronous oscillation events," in *CIGRE US National Committee 2018 Grid of the Future Symposium*, 2018.
- [5] L. Wang, X. Xie, Q. Jiang, et al., "Investigation of SSR in Practical DFIG-Based Wind Farms Connected to a Series-Compensated Power System," *IEEE Trans. Power Syst.*, vol. 30, no. 5, pp. 2772–2779, Sept. 2015.
- [6] G. D. Irwin, A. K. Jindal and A. L. Isaacs, "Sub-synchronous control interactions between type 3 wind turbines and series compensated AC transmission systems," in *2011 IEEE Power and Energy Society General Meeting*, Detroit, MI, USA, 2011, pp. 1–6.
- [7] L. C. Gross, "Sub-synchronous grid conditions: New event, new problem, and new solutions," in *Proc. Western Protective Relay Conf.*, Oct. 2010, pp. 1–5.
- [8] L. Fan, R. Kavasseri, Z. L. Miao et al., "Modeling of DFIG-Based Wind Farms for SSR Analysis," *IEEE Trans. Power Deliv.*, vol. 25, no. 4, pp. 2073–2082, Oct. 2010.
- [9] IEEE PES WindSSO Taskforce, "PES TR-80: Wind Energy Systems Subynchronous Oscillations: Events and Modeling," Oct. 2020. [https://resourcecenter.ieee-pes.org/publications/technical-reports/PES\\_TP\\_TR80](https://resourcecenter.ieee-pes.org/publications/technical-reports/PES_TP_TR80).
- [10] A. Chen, D. Xie, D. Zhang, et al., "PI Parameter Tuning of Converters for Sub-Synchronous Interactions Existing in Grid-Connected DFIG Wind Turbines," *IEEE Trans. Power Electron.*, vol. 34, no. 7, pp. 6345–6355, July 2019.
- [11] M. T. Ali, D. Zhou, Y. Song, et al., "Analysis and Mitigation of SSCI in DFIG Systems With Experimental Validation," *IEEE Trans. Energy Convers.*, vol. 35, no. 2, pp. 714–723, June 2020.
- [12] S. Chernet, M. Bongiorno, G. K. Andersen, et al., "Online variation of wind turbine controller parameter for mitigation of SSR in DFIG based wind farms," in *2016 IEEE Energy Conversion Congress and Exposition (ECCE)*, Milwaukee, WI, USA, Sept. 2016, pp. 1–8.
- [13] X. Wu, Y. Guan, X. Yang, et al., "Low-cost control strategy based on reactive power regulation of DFIG-based wind farm for SSO suppression," *IET Renew. Power Gener.*, vol. 13, no. 1, pp. 33–39, Jan. 2019.
- [14] L. Harnefors, M. Bongiorno and S. Lundberg, "Input-Admittance Calculation and Shaping for Controlled Voltage-Source Converters," *IEEE Trans. Ind. Electron.*, vol. 54, no. 6, pp. 3323–3334, Dec. 2007.
- [15] S. Golestan, M. Monfared and F. D. Freijedo, "Design-Oriented Study of Advanced Synchronous Reference Frame Phase-Locked Loops," *IEEE Trans. Power Electron.*, vol. 28, no. 2, pp. 765–778, Feb. 2013.
- [16] B. -H. Kim and S. -K. Sul, "Shaping of PWM Converter Admittance for Stabilizing Local Electric Power Systems," *IEEE Open J. Power Electron.*, vol. 4, no. 4, pp. 1452–1461, Dec. 2016.
- [17] S. Zhou et al., "An Improved Design of Current Controller for LCL-Type Grid-Connected Converter to Reduce Negative Effect of PLL in Weak Grid," *IEEE Open J. Power Electron.*, vol. 6, no. 2, pp. 648–663, Jun. 2018.
- [18] D. Zhu, S. Zhou, X. Zou and Y. Kang, "Improved Design of PLL Controller for LCL-Type Grid-Connected Converter in Weak Grid," *IEEE Trans. Power Electron.*, vol. 35, no. 5, pp. 4715–4727, May 2020.
- [19] H. A. Mohammadpour and E. Santi, "Analysis of subsynchronous control interactions in DFIG-based wind farms: ERCOT case study," in *2015 IEEE Energy Conversion Congress and Exposition (ECCE)*, Montreal, QC, Canada, 2015, pp. 500–505.
- [20] I. Vieto and J. Sun, "Damping of subsynchronous resonance involving Type-III wind turbines," in *2015 IEEE 16th Workshop on Control and Modeling for Power Electronics (COMPEL)*, Vancouver, BC, Canada, Jul. 2015, pp. 1–8.
- [21] M. A. Chowdhury and M. A. Mahmud, "Mitigation of subsynchronous control interaction in series-compensated DFIG-based wind farms using a nonlinear partial feedback linearizing controller," in *2016 IEEE*

> REPLACE THIS LINE WITH YOUR MANUSCRIPT ID NUMBER (DOUBLE-CLICK HERE TO EDIT) <

- Innovative Smart Grid Technologies - Asia (ISGT-Asia)*, Melbourne, VIC, Australia, 2016, pp. 335-340.
- [22] L. Wang, X. Xie, Q. Jiang, et al., "Centralised solution for subsynchronous control interaction of doubly fed induction generators using voltage-sourced converter," *IET gener., transm. & distri.*, vol. 9, no. 16, pp. 2751-2759, Aug. 2015.
- [23] V. B. Virulkar and G. V. Gotmare, "Sub-synchronous resonance in series compensated wind farm: A review," *Renew. Sustain. Energy Rev.*, vol. 55, pp. 1010-1029, Dec. 2015.
- [24] J. Shair, X. Xie and G. Yan, "Mitigating subsynchronous control interaction in wind power systems: Existing techniques and open challenges," *Renew. Sustain. Energy Rev.*, vol. 108, pp. 330-346, Jul. 2019.
- [25] N. Verma, N. Kumar, S. Gupta, et al., "Review of sub-synchronous interaction in wind integrated power systems: classification, challenges, and mitigation techniques," *Protection and control of modern power systems*, vol. 8, no. 1, pp. 1-26, Apr. 2023.
- [26] IEEE Committee Report, "Reader's guide to sub-synchronous resonance," *IEEE Trans. Power Syst.*, Vol. 7, No. 1, pp. 150-157, Feb. 1992.
- [27] L. Fan, R. Kavasseri, Z. L. Miao and C. Zhu, "Modeling of DFIG-Based Wind Farms for SSR Analysis," *IEEE Trans. Power Deliv.*, vol. 25, no. 4, pp. 2073-2082, Oct. 2010.
- [28] U. Karaagac, J. Mahseredjian, S. Jensen, et al., "Safe Operation of DFIG-Based Wind Parks in Series-Compensated Systems," *IEEE Trans. Power Deliv.*, vol. 33, no. 2, pp. 709-718, Apr. 2018.
- [29] P. Kundur, *Power system stability and control*. New York: New York: McGraw-Hill, 1994.
- [30] C. Zhu, L. Fan and M. Hu, "Control and analysis of DFIG-based wind turbines in a series compensated network for SSR damping," in *IEEE PES General Meeting*, Minneapolis, MN, USA, Jul. 2010.
- [31] L. Fan and Z. Miao, "Mitigating SSR Using DFIG-Based Wind Generation," *IEEE Trans. Sustain. Energy*, vol. 3, no. 3, pp. 349-358, July 2012.
- [32] H. A. Mohammadpour and E. Santi, "SSR Damping Controller Design and Optimal Placement in Rotor-Side and Grid-Side Converters of Series-Compensated DFIG-Based Wind Farm," *IEEE Trans. Sustain. Energy*, vol. 6, no. 2, pp. 388-399, Apr. 2015.
- [33] M. T. Ali, M. Ghandhari and L. Harnefors, "Mitigation of sub-synchronous control interaction in DFIGs using a power oscillation damper," in *2017 IEEE Manchester PowerTech*, Manchester, UK, 2017, pp. 1-6.
- [34] G. Rogers, *Power System Oscillations*. Norwell, MA: Kluwer, Dec. 1999.
- [35] A. E. Leon and J. A. Solsona, "Sub-Synchronous Interaction Damping Control for DFIG Wind Turbines," *IEEE Trans. Power Syst.*, vol. 30, no. 1, pp. 419-428, Jan. 2015.
- [36] A. E. Leon, "Integration of DFIG-Based Wind Farms Into Series-Compensated Transmission Systems," *IEEE Trans. Sustain. Energy*, vol. 7, no. 2, pp. 451-460, Apr. 2016.
- [37] Z. Wu, C. Zhu, and M. Hu, "Supplementary Controller Design for SSR Damping in a Series-Compensated DFIG-Based Wind Farm," *Energies (Basel)*, vol. 5, no. 11, pp. 4481-4496, Nov. 2012.
- [38] H. A. Mohammadpour and E. Santi, "Analysis of subsynchronous control interactions in DFIG-based wind farms: ERCOT case study," in *2015 IEEE Energy Conversion Congress and Exposition (ECCE)*, Montreal, QC, Canada, 2015, pp. 500-505.
- [39] "Technical Connection Rules for High-Voltage (VDE-AR-N 4120)," Berlin, Germany: VDE VERLAG GMBH, Nov. 2018. [Online]. Available: <https://www.vde.com/en/fnn/topics/technical-connection-rules/tar-for-high-voltage>.
- [40] M. Ghafouri, U. Karaagac, H. Karimi, S. Jensen, J. Mahseredjian and S. O. Faried, "An LQR Controller for Damping of Subsynchronous Interaction in DFIG-Based Wind Farms," *IEEE Trans. Power Syst.*, vol. 32, no. 6, pp. 4934-4942, Nov. 2017.
- [41] U. Karaagac, S. O. Faried, J. Mahseredjian, and A. A. Edris, "Coordinated control of wind energy conversion systems for mitigating subsynchronous interaction in DFIG-based wind farms," *IEEE Trans. Smart Grid*, vol. 5, no. 5, pp. 2440-2449, Sep. 2014.
- [42] D. Zhu, X. Zou, L. Deng, Q. Huang, S. Zhou and Y. Kang, "Inductance-Emulating Control for DFIG-Based Wind Turbine to Ride-Through Grid Faults," *IEEE Trans. Power Electron.*, vol. 32, no. 11, pp. 8514-8525, Nov. 2017.
- [43] D. Zhu, X. Zou, S. Zhou, W. Dong, Y. Kang and J. Hu, "Feedforward Current References Control for DFIG-Based Wind Turbine to Improve Transient Control Performance During Grid Faults," *IEEE Trans. Energy Convers.*, vol. 33, no. 2, pp. 670-681, Jun. 2018.
- [44] Y. Chang, M. Berger and I. Kocar, "Control Solution to Over-Modulation of DFIG Converter for Asymmetrical Fault Ride Through," *IEEE Trans. Sustain. Energy*, vol. 15, no. 1, pp. 703-706, Jan. 2024.
- [45] Y. Seyedi, U. Karaagac, J. Mahseredjian, A. Haddadi, K. Jacobs, H. Karimi, "Detailed modeling of inverter-based resources", in *Advances in power system modeling, control and stability analysis*, 2nd ed. IET Energy Engineering, 2022, pp. 175-203 [Chapter 5].
- [46] M. Ghafouri, U. Karaagac, I. Kocar, Z. Xu and E. Farantatos, "Analysis and Mitigation of the Communication Delay Impacts on Wind Farm Central SSI Damping Controller," *IEEE Access*, vol. 9, pp. 105641-105650, Jul. 2021.
- [47] M. Ghafouri, U. Karaagac, J. Mahseredjian and H. Karimi, "SSCI Damping Controller Design for Series-Compensated DFIG-Based Wind Parks Considering Implementation Challenges," *IEEE Trans. Power Syst.*, vol. 34, no. 4, pp. 2644-2653, July 2019.
- [48] M. Ghafouri, U. Karaagac, A. Ameli, J. Yan and C. Assi, "A Cyber Attack Mitigation Scheme for Series Compensated DFIG-Based Wind Parks," *IEEE Trans. Smart Grid*, vol. 12, no. 6, pp. 5221-5232, Nov. 2021.
- [49] J. Yao, X. Wang, J. Li, R. Liu and H. Zhang, "Sub-Synchronous Resonance Damping Control for Series-Compensated DFIG-Based Wind Farm With Improved Particle Swarm Optimization Algorithm," *IEEE Trans. Energy Convers.*, vol. 34, no. 2, pp. 849-859, June 2019.
- [50] H. A. Mohammadpour and E. Santi, "Optimal adaptive sub-synchronous resonance damping controller for a series-compensated doubly-fed induction generator-based wind farm," *IET renew. power gener.*, vol. 9, no. 6, pp. 669-681, Feb. 2015.
- [51] M. T. Ali, M. Ghandhari and L. Harnefors, "Mitigation of sub-synchronous control interaction in DFIGs using a power oscillation damper," in *2017 IEEE Manchester PowerTech*, Manchester, UK, 2017.
- [52] X. Bian, Y. Ding, Q. Jia, L. Shi, X.-P. Zhang, and K. L. Lo, "Mitigation of sub-synchronous control interaction of a power system with DFIG-based wind farm under multi-operating points," *IET gener., transm. & distri.*, vol. 12, no. 21, pp. 5834-5842, Sept. 2018.
- [53] X. Wu, W. Ning, T. Yin, X. Yang and Z. Tang, "Robust Design Method for the SSDC of a DFIG Based on the Practical Small-Signal Stability Region Considering Multiple Uncertainties," *IEEE Access*, vol. 6, pp. 16696-16703, Apr. 2018.
- [54] H. Ghaffarzadeh and A. Mehrizi-Sani, "Mitigation of Subsynchronous Resonance Induced by a Type III Wind System," *IEEE Trans. Sustain. Energy*, vol. 11, no. 3, pp. 1717-1727, July 2020.
- [55] K. Ogata, *Modern Control Engineering*. Englewood Cliffs, NJ, USA: Prentice Hall, 1997.
- [56] M.G. Safonov, R.Y. Chiang, "A Schur Method for Balanced Model Reduction," *IEEE Trans. on Automat. Contr.*, 34 (1989) 729-733.
- [57] H. A. Mohammadpour, A. Ghaderi, H. Mohammadpour, and E. Santi., "SSR damping in wind farms using observed-state feedback control of DFIG converters," *Electr. power syst. Res.*, vol. 123, pp. 57-66, Feb. 2015.
- [58] I. Vieto and J. Sun, "Damping of subsynchronous resonance involving Type-III wind turbines," in *2015 IEEE 16th Workshop on Control and Modeling for Power Electronics (COMPEL)*, Vancouver, BC, Canada, Jul. 2015, pp. 1-8.
- [59] P. -H. Huang, M. S. El Moursi, W. Xiao and J. L. Kirtley, "Subsynchronous Resonance Mitigation for Series-Compensated DFIG-Based Wind Farm by Using Two-Degree-of-Freedom Control Strategy," *IEEE Trans. Power Syst.*, vol. 30, no. 3, pp. 1442-1454, May 2015.
- [60] H. Liu, X. Xie, Y. Li, H. Liu and Y. Li, "Damping DFIG-associated SSR with subsynchronous suppression filters: A case study on a practical wind farm system," in *International Conference on Renewable Power Generation (RPG 2015)*, Beijing, Oct. 2015.
- [61] H. Liu, X. Xie, Y. Li, H. Liu and Y. Hu, "Damping subsynchronous resonance in series-compensated wind farms by adding notch filters to DFIG controllers," in *2015 IEEE Innovative Smart Grid Technologies - Asia (ISGT ASIA)*, Bangkok, Thailand, Nov. 2015, pp. 1-5.
- [62] H. Liu, X. Xie, J. He, H. Liu and Y. Li, "Damping DFIG-associated SSR by adding subsynchronous suppression filters to DFIG converter controllers," in *2016 IEEE Power and Energy Society General Meeting (PESGM)*, Boston, MA, Jul. 2016, pp. 1-5.

> REPLACE THIS LINE WITH YOUR MANUSCRIPT ID NUMBER (DOUBLE-CLICK HERE TO EDIT) <

- [63] W. Ning, X. Wu, Y. Guan and F. Chen, "Method to suppress sub-synchronous oscillation of DFIG-based wind farms based on virtual impedance," *The Journal of Engineering*, vol. 2017, no. 13, pp. 2173-2177, Jan. 2018.
- [64] Y. Meng, X. Pan, H. Ma, et al, "Analysis and mitigation of sub-synchronous resonance based on integral control for DFIG-based wind farm," *IET gener., transm. & distri.*, vol. 13, no. 9, pp. 1718-1725, Apr. 2019.
- [65] Y. Li, L. Fan et al., "Replicating Real-World Wind Farm SSR Events," *IEEE Trans. Power Deliv.*, vol. 35, no. 1, pp. 339-348, Feb. 2020.
- [66] J. Shair, X. Xie, Y. Li and V. Terzija, "Hardware-in-the-Loop and Field Validation of a Rotor-Side Subsynchronous Damping Controller for a Series Compensated DFIG System," *IEEE Trans. Power Deliv.*, vol. 36, no. 2, pp. 698-709, Apr. 2021.
- [67] F. Meng, D. Sun, K. Zhou, J. Wu, F. Zhao and L. Sun, "A Sub-Synchronous Oscillation Suppression Strategy for Doubly Fed Wind Power Generation System," *IEEE Access*, vol. 9, pp. 83482-83498, Jun. 2021.
- [68] X. Tian, Y. Chi, Y. Li, H. Tang, C. Liu and Y. Su, "Coordinated damping optimization control of sub-synchronous oscillation for DFIG and SVG," *CSEE J. Power and Energy Syst.*, vol. 7, no. 1, pp. 140-149, Jan. 2021.
- [69] M. A. Chowdhury, M. A. Mahmud, W. Shen and H. R. Pota, "Nonlinear Controller Design for Series-Compensated DFIG-Based Wind Farms to Mitigate Subsynchronous Control Interaction," *IEEE Trans. Energy Convers.*, vol. 32, no. 2, pp. 707-719, Jun. 2017.
- [70] Y. Wang, Q. Wu, R. Yang, et al., "H $\infty$  current damping control of DFIG based wind farm for sub-synchronous control interaction mitigation," *Int. J. Electr. Power & Energy Syst.*, vol. 98, pp. 509-519, Jan. 2018.
- [71] P. Li, J. Wang, F. Wu, and H. Li, "Nonlinear controller based on state feedback linearization for series-compensated DFIG-based wind power plants to mitigate sub-synchronous control interaction," *Int. Trans. Electr.*, vol. 29, no. 1, pp. 1-23, 2019.
- [72] P. Li, L. Xiong, F. Wu, M. Ma, and J. Wang, "Sliding mode controller based on feedback linearization for damping of sub-synchronous control interaction in DFIG-based wind power plants," *Int. J. Electr. Power & Energy Syst.*, vol. 107, pp. 239-250, May 2019.
- [73] P. Li, J. Wang, L. Xiong and M. Ma, "Robust Nonlinear Controller Design for Damping of Sub-Synchronous Control Interaction in DFIG-Based Wind Farms," *IEEE Access*, vol. 7, pp. 16626-16637, Feb. 2019.
- [74] M. Ghafouri, U. Karaagac, H. Karimi and J. Mahseredjian, "Robust subsynchronous interaction damping controller for DFIG-based wind farms," *J. Mod. Power Syst. Clean Energy*, vol. 7, no. 6, pp. 1663-1674, Nov. 2019.
- [75] Q. Li, Y. Hu, Y. Wang, C. Zhou, Y. Li and J. Han, "Design and Simulation of a Novel Subsynchronous Control Interaction Damping Controller," in *2020 Asia Energy and Electrical Engineering Symposium (AEEES)*, Chengdu, China, May 2020.
- [76] C. Karunanayake, J. Ravishanker and Z. Y. Dong, "Nonlinear SSR Damping Controller for DFIG Based Wind Generators Interfaced to Series Compensated Transmission Systems," *IEEE Trans. Power Syst.*, vol. 35, no. 2, pp. 1156-1165, Mar. 2020.
- [77] P. Li, J. Wang, L. Xiong, S. Huang, M. Ma and Z. Wang, "Energy-Shaping Controller for DFIG-Based Wind Farm to Mitigate Subsynchronous Control Interaction," *IEEE Trans. Power Syst.*, vol. 36, no. 4, pp. 2975-2991, Jul. 2021.
- [78] R. K. Varma and S. Auddy, "Mitigation of subsynchronous oscillations in a series compensated wind farm with static var compensator," in *2006 IEEE Power Engineering Society General Meeting*, Montreal, QC, Canada, 2006, pp. 1-7.
- [79] R. K. Varma, S. Auddy and Y. Semsedini, "Mitigation of Subsynchronous Resonance in a Series-Compensated Wind Farm Using FACTS Controllers," *IEEE Trans. Power Deliv.*, vol. 23, no. 3, pp. 1645-1654, July 2008.
- [80] M. S. El-Moursi, B. Bak-Jensen and M. H. Abdel-Rahman, "Novel STATCOM Controller for Mitigating SSR and Damping Power System Oscillations in a Series Compensated Wind Park," *IEEE Trans. Power Electron.*, vol. 25, no. 2, pp. 429-441, Feb. 2010.
- [81] A. Moharana, R. K. Varma and R. Seethapathy, "SSR Alleviation by STATCOM in Induction-Generator-Based Wind Farm Connected to Series Compensated Line," *IEEE Trans. Sustain. Energy*, vol. 5, no. 3, pp. 947-957, July 2014.
- [82] R. K. Varma, Y. Semsedini and S. Auddy, "Mitigation of subsynchronous oscillations in a series compensated wind farm with Thyristor Controlled Series Capacitor (TCSC)," in *2007 Power Systems Conference: Advanced Metering, Protection, Control, Communication, and Distributed Resources*, Clemson, SC, USA, 2007, pp. 331-337.
- [83] H. A. Mohammadpour, M. M. Islam, E. Santi and Y. -J. Shin, "SSR Damping in Fixed-Speed Wind Farms Using Series FACTS Controllers," *IEEE Trans. Power Deliv.*, vol. 31, no. 1, pp. 76-86, Feb. 2016.
- [84] L. Wang, X. Xie, Q. Jiang, and X. Liu, "Centralised solution for subsynchronous control interaction of doubly fed induction generators using voltage-sourced converter," *IET gener., transm. Distri.*, vol. 9, no. 16, pp. 2751-2759, Aug. 2015.
- [85] S. Golshannavaz, F. Aminifar and D. Nazarpour, "Application of UPFC to Enhancing Oscillatory Response of Series-Compensated Wind Farm Integrations," *IEEE Trans. Smart Grid*, vol. 5, no. 4, pp. 1961-1968, July 2014.
- [86] X. Zhang, X. Xie, H. Liu, and Y. Li, "Robust subsynchronous damping control to stabilise SSR in series-compensated wind power systems," *IET gener., transm. Distri.*, vol. 13, no. 3, pp. 337-344, Jan. 2019.
- [87] X. Zhang, X. Xie, J. Shair, H. Liu, Y. Li and Y. Li, "A Grid-Side Subsynchronous Damping Controller to Mitigate Unstable SSCI and Its Hardware-in-the-loop Tests," *IEEE Trans. Sustain. Energy*, vol. 11, no. 3, pp. 1548-1558, July 2020.
- [88] A. E. Leon and J. M. Mauricio, "Mitigation of Subsynchronous Control Interactions Using Multi-Terminal DC Systems," *IEEE Trans. Sustain. Energy*, vol. 12, no. 1, pp. 420-429, Jan. 2021.
- [89] P. Dattaray, P. Wall and V. Terzija, "Subsynchronous Control Interaction Damping using Colocated BESS in Large Wind Farms," in *2021 IEEE Madrid PowerTech*, Madrid, Spain, Jun. 2021, pp. 1-6.
- [90] F. Salehi, A. Golshani, I. B. M. Matsuo, et al., "On Mitigation of Sub-Synchronous Control Interactions in Hybrid Generation Resources," *IEEE Trans. Ind.*, vol. 18, no. 7, pp. 4372-4382, July 2022.
- [91] D. H. R. Suriyaarachchi, U. D. Annakkage, C. Karawita, et al., "Application of an SVC to damp sub-synchronous interaction between wind farms and series compensated transmission lines," in *2012 IEEE Power and Energy Society General Meeting*, San Diego, CA, USA, 2012, pp. 1-6.
- [92] H. Xie and M. M. de Oliveira, "Mitigation of SSR in presence of wind power and series compensation by SVC," in *2014 International Conference on Power System Technology*, Chengdu, China, 2014, pp. 2819-2826.
- [93] X. Zhang, X. Xie, H. Liu, H. Liu, Y. Li, and C. Zhang, "Mitigation of Sub-Synchronous Control Interaction in Wind Power systems with GA-SA tuned Damping Controller," in *IFAC-PapersOnLine*, Vol. 50, No. 1, Jul. 2017.
- [94] L. Wang, J. Peng, Y. You, and H. Ma, "SSCI performance of DFIG with direct controller," *IET gener., transm. Distri.*, vol. 11, no. 10, pp. 2697-2702, Jun. 2017.
- [95] W. Yan, S. Shah, V. Gevorgian, P. Koralewicz and R. Wallen, "On the low risk of SSR in type III wind turbines operating in grid-forming control," in *21st Wind & Solar Integration Workshop (WIW 2022)*, Hybrid Conference, The Hague, Netherlands, 2022, pp. 74-79.
- [96] F. Meng, D. Sun, K. Zhou, J. Wu, F. Zhao and L. Sun, "A Sub-Synchronous Oscillation Suppression Strategy for Doubly Fed Wind Power Generation System," *IEEE Access*, vol. 9, pp. 83482-83498, Jun. 2021.
- [97] Y. Gu, J. Liu, T. C.Green, W. Li, and X. He, "Motion-induction compensation to mitigate sub-synchronous oscillation in wind farms," *IEEE Trans. Sustain. Energy*, vol. 11, no. 3, pp. 1247-1256, Jul. 2020.
- [98] A. E. Leon, S. J. Amodeo, and J. M. Mauricio, "Enhanced Compensation Filter to Mitigate Subsynchronous Oscillations in Series-Compensated DFIG-Based Wind Farms," *IEEE Trans. Power Deliv.*, vol. 36, no. 6, pp. 3805-3814, Dec. 2021.
- [99] L. J. Cai, I. Erlich, U. Karaagac, and J. Mahseredjian, "Stable operation of doubly-fed induction generator in weak grids," *IEEE Power and Energy Society General Meeting*, Sep. 2015.
- [100] L. J. Cai and I. Erlich, "Doubly Fed Induction Generator Controller Design for the Stable Operation in Weak Grids," *IEEE Trans. Sustain. Energy*, vol. 6, no. 3, pp. 1078-1084, Jul. 2015.
- [101] I. Vieto, G. Li, and J. Sun, "Behavior, Modeling and Damping of a New Type of Resonance Involving Type-III Wind Turbines," in *2018 IEEE 19th Workshop on Control and Modeling for Power Electronics, COMPEL 2018*, Sep. 2018.
- [102] J. Sun and I. Vieto, "Development and Application of Type-III Turbine Impedance Models Including DC Bus Dynamics," *IEEE Open J. Power Electron.*, vol. 1, pp. 513-528, Nov. 2020.

> REPLACE THIS LINE WITH YOUR MANUSCRIPT ID NUMBER (DOUBLE-CLICK HERE TO EDIT) <

- [103] A. Husham, I. Kamwa, M. A. Abido and H. Suprême, "Decentralized Stability Enhancement of DFIG-Based Wind Farms in Large Power Systems: Koopman Theoretic Approach," *IEEE Access*, vol. 10, pp. 27684-27697, 2022.
- [104] A. Brosch, S. Hanke, O. Wallscheid and J. Böcker, "Data-Driven Recursive Least Squares Estimation for Model Predictive Current Control of Permanent Magnet Synchronous Motors," *IEEE Trans. Power Electron.*, vol. 36, no. 2, pp. 2179-2190, Feb. 2021.
- [105] S. Wang, T. Dragicevic, G. F. Gontijo, S. K. Chaudhary and R. Teodorescu, "Machine Learning Emulation of Model Predictive Control for Modular Multilevel Converters," *IEEE Trans. Ind. Electron.*, vol. 68, no. 11, pp. 11628-11634, Nov. 2021.
- [106] R. Yousefian, R. Bhattarai and S. Kamalasadani, "Transient Stability Enhancement of Power Grid With Integrated Wide Area Control of Wind Farms and Synchronous Generators," *IEEE Trans. Power Syst.*, vol. 32, no. 6, pp. 4818-4831, Nov. 2017.
- [107] L. Zhou, A. Swain and A. Ukil, "Reinforcement Learning Controllers for Enhancement of Low Voltage Ride Through Capability in Hybrid Power Systems," *IEEE Trans. Ind. Inform.*, vol. 16, no. 8, pp. 5023-5031, Aug. 2020.
- [108] N. T. -T. Vu, H. D. Nguyen and A. T. Nguyen, "Reinforcement Learning-Based Adaptive Optimal Fuzzy MPPT Control for Variable Speed Wind Turbine," *IEEE Access*, vol. 10, pp. 95771-95780, 2022.
- [109] T. P. Lillicrap et al, "Continuous control with deep reinforcement learning," arxiv: 1509.02971, <https://arxiv.org/abs/1509.02971>, 2015.
- [110] T. Xue, U. Karaagac, I. Kocar, M. B. Vavdareh and M. Ghafouri, "Machine Learning Basics and Potential Applications in Power Systems," in *2023 International Conference on Electrical, Communication and Computer Engineering (ICECCE)*, Dubai, United Arab Emirates, Dec. 2023, pp. 1-7.
- [111] D. Ernst, M. Glavic and L. Wehenkel, "Power systems stability control: reinforcement learning framework," *IEEE Trans. Power Syst.*, vol. 19, no. 1, pp. 427-435, Feb. 2004.
- [112] D. Ernst and L. Wehenkel, "FACTS Devices Controlled by Means of Reinforcement Learning Algorithms," in *Proc. Power Syst. Comput. Conf. Sevilla*, Spain, Jun. 2002.
- [113] M. Glavic, D. Ernst, L. Wehenkel, "A Reinforcement Learning Based Discrete Supplementary Control for Power System Transient Stability Enhancement," *International Journal of Engineering Intelligent Systems for Electrical Engineering and Communications*, vol. 13, no. 2, 2005.
- [114] R. Hadidi and B. Jeyasurya, "Reinforcement learning approach for controlling power system stabilizers," *Canadian journal of electrical and computer engineering*, vol. 34, no. 3, pp. 99-103, 2009.
- [115] R. Hadidi and B. Jeyasurya, "Reinforcement Learning Based Real-Time Wide-Area Stabilizing Control Agents to Enhance Power System Stability," *IEEE Trans. Smart Grid*, vol. 4, no. 1, pp. 489-497, Mar. 2013.
- [116] J. Duan, H. Xu and W. Liu, "Q-Learning-Based Damping Control of Wide-Area Power Systems Under Cyber Uncertainties," *IEEE Trans. Smart Grid*, vol. 9, no. 6, pp. 6408-6418, Nov. 2018.
- [117] I. Goodfellow, Y. Bengio, and A. Courville, *Deep Learning*. Cambridge, MA, USA: MIT Press, 2016.
- [118] Y. Hashmy, Z. Yu, D. Shi and Y. Weng, "Wide-Area Measurement System-Based Low Frequency Oscillation Damping Control Through Reinforcement Learning," *IEEE Trans. Smart Grid*, vol. 11, no. 6, pp. 5072-5083, Nov. 2020.
- [119] G. Zhang et al., "Deep Reinforcement Learning-Based Approach for Proportional Resonance Power System Stabilizer to Prevent Ultra-Low-Frequency Oscillations," *IEEE Trans. Smart Grid*, vol. 11, no. 6, pp. 5260-5272, Nov. 2020.
- [120] G. Zhang, W. Hu, J. Zhao, D. Cao, Z. Chen and F. Blaabjerg, "A Novel Deep Reinforcement Learning Enabled Multi-Band PSS for Multi-Mode Oscillation Control," *IEEE Trans. Power Systems*, vol. 36, no. 4, pp. 3794-3797, July 2021.
- [121] G. Zhang et al., "A Multiagent Deep Reinforcement Learning-Enabled Dual-Branch Damping Controller for Multimode Oscillation," *IEEE Trans. Control Syst. Technol.*, vol. 31, no. 1, pp. 483-492, Jan. 2023.
- [122] P. Gupta, A. Pal and V. Vittal, "Coordinated Wide-Area Damping Control Using Deep Neural Networks and Reinforcement Learning," *IEEE Trans. Power Syst.*, vol. 37, no. 1, pp. 365-376, Jan. 2022.
- [123] Y. Liu, S. Gao, G. Qiu, T. Liu, L. Ding and J. Liu, "A Physics-Informed Action Network for Transient Stability Preventive Control," *IEEE Trans. Power Syst.*, vol. 38, no. 2, pp. 1771-1774, Mar. 2023.



**Tao Xue** (Member, IEEE) received the B.Eng. and M.Eng. degrees in EEE from the North China Electric Power University (Beijing) and Shanghai Jiao Tong University, China, in 2018 and 2021, respectively, and the Ph.D. degree in EEE from The Hong Kong Polytechnic University, Hong Kong, in 2024.

He is currently a Research Associate (postdoc) at the Department of Electrical and Electronic Engineering, The Hong Kong Polytechnic University. Tao Xue's research interests include stability analysis, damping controller design, fast simulations and machine learning applications in future power systems.



**Ulas Karaagac** (Member, IEEE) received the B.Sc. and M.Sc. degrees in electrical and electronics engineering from the Orta Doğu Teknik Üniversitesi, Ankara, Turkey, in 1999 and 2002, respectively, and the Ph.D. degree in electrical engineering from Polytechnique Montréal, Montreal, QC, Canada, in 2011.

He was a Research and Development Engineer with the Information Technology and Electronics Research Institute (BILTEN), Scientific and Technical Research Council of Turkey (TUBITAK), from 1999 to 2007. He was also a Postdoctoral Fellow (2011 – 2013) and a Research Associate (2013 – 2016) with Polytechnique Montréal. He was an Assistant Professor of the Department of Electrical Engineering, The Hong Kong Polytechnic University, from 2016 to 2023. He is currently a Lecturer of the Department of Electrical and Electronics Engineering, Orta Doğu Teknik Üniversitesi. His research interests include integration of largescale renewables into power grids, modeling and simulation of large-scale power systems, and power system dynamics and control.



**Mohsen Ghafouri** (Member, IEEE) received the B.Sc. and master's degrees in electrical engineering from the Sharif University of Technology, Tehran, Iran, in 2009 and 2011, respectively, and the Ph.D. degree in electrical engineering from Polytechnique Montreal, Montreal, QC, Canada, in 2018.

He was a Researcher with the Iranian Power System Research Institute, Sharif University of Technology, from 2011 to 2014. In 2018, he was a Researcher with the CYME International, Eaton Power System Solutions, Montreal. In August 2018, he joined the Security Research Group, Concordia University, Montreal, as a Horizon Postdoctoral Fellow, where he is currently an Assistant Professor. His research interests include cyber-security of smart grids, power system modeling, microgrid, wind energy, and control of industrial processes.



**İlhan Kocar** (Senior Member, IEEE) received the B.Sc. and M.Sc. degrees in EEE from Orta Doğu Teknik Üniversitesi, Ankara, Turkey, in 1998 and 2003, respectively, and the Ph.D. degree in EE from École Polytechnique de Montréal (affiliated with Université de Montréal), QC, Canada, in 2009.

He has 25 years of diverse experience in the power engineering field across industry, academia, and major regions including North America, Asia, and Europe. He is now a full professor at Polytechnique Montréal. His research aims to address critical challenges in integrating renewable energy sources into power systems. He is an Editor of IEEE Transactions on Power Delivery and

Journal of Modern Power Systems and Clean Energy.